Provided for non-commercial research and educational use only.
Not for reproduction or distribution or commercial use.

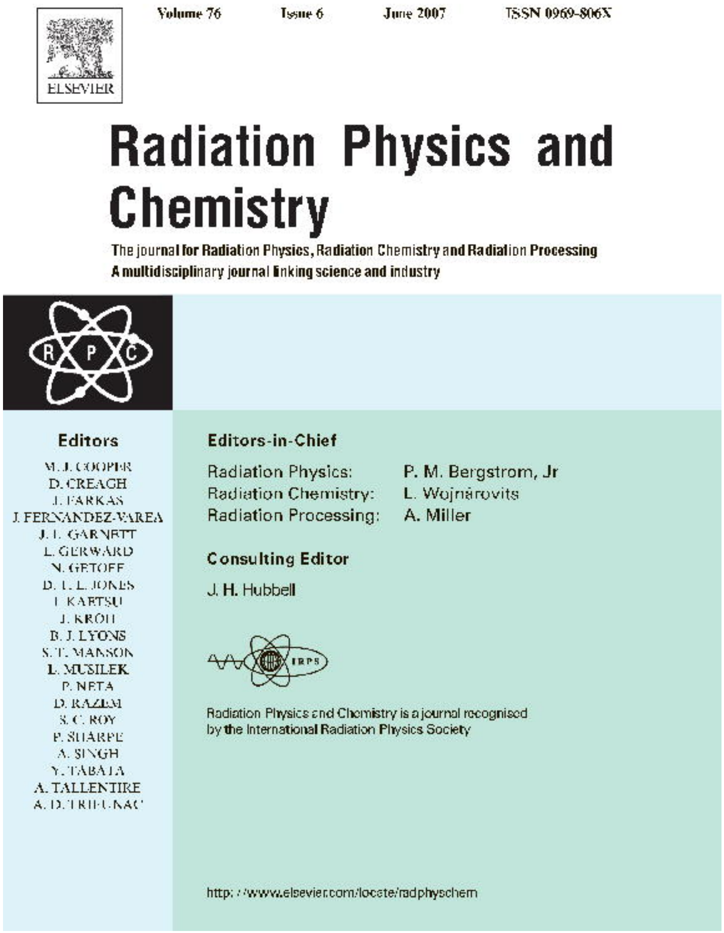

Volume 76 Issue 6 June 2007 ISSN 0969-806X

ELSEVIER

Radiation Physics and Chemistry

The journal for Radiation Physics, Radiation Chemistry and Radiation Processing
A multidisciplinary journal linking science and industry

Editors

M. J. COOPER
D. CREAGH
J. FARKAS
J. FERNANDEZ-VAREA
J. L. GARNETT
L. GERWARD
N. GETOFF
D. T. L. JONES
I. KAETSU
J. KROH
B. J. LYONS
S. T. MANSON
L. MUSILEK
P. NETA
D. RAZEM
S. C. ROY
P. SHARPE
A. SINGH
Y. TABATA
A. TALLENTIRE
A. D. TRIFUNAC

Editors-in-Chief

Radiation Physics: P. M. Bergstrom, Jr
Radiation Chemistry: L. Wojnárovits
Radiation Processing: A. Miller

Consulting Editor

J. H. Hubbell

Radiation Physics and Chemistry is a journal recognised by the International Radiation Physics Society

http://www.elsevier.com/locate/radphyschem

This article was originally published in a journal published by Elsevier, and the attached copy is provided by Elsevier for the author's benefit and for the benefit of the author's institution, for non-commercial research and educational use including without limitation use in instruction at your institution, sending it to specific colleagues that you know, and providing a copy to your institution's administrator.

All other uses, reproduction and distribution, including without limitation commercial reprints, selling or licensing copies or access, or posting on open internet sites, your personal or institution's website or repository, are prohibited. For exceptions, permission may be sought for such use through Elsevier's permissions site at:

http://www.elsevier.com/locate/permissionusematerial

Available online at www.sciencedirect.com
ScienceDirect
Radiation Physics and Chemistry 76 (2007) 998–1010
Radiation Physics and Chemistry
www.elsevier.com/locate/radphyschem

Experimental and computer simulation study of delayed fluorescence decay from irradiated *n*-dodecane solutions of TMPD

V.I. Borovkov[a,b,*], K.A. Velizhanin[b]

[a] *Institute of Chemical Kinetics and Combustion, SB RAS, Novosibirsk 630090, Russian Federation*
[b] *Novosibirsk State University, Novosibirsk 630090, Russian Federation*

Received 21 July 2006; accepted 27 September 2006

Abstract

A computer model of the formation of molecular excited states in irradiated alkane solutions was applied successfully to the analysis of the experimental delayed fluorescence decays measured in the range 0–250 ns after X-ray pulsed irradiation of *n*-dodecane solutions of *N,N,N′,N′*-tetramethyl-*para*-phenylenediamine (TMPD). The modeling demonstrated that a track produced by 20-keV X-ray quanta in *n*-dodecane in the studied time range could be described by a set of isolated spherical spurs containing 4–5 ion pairs. The radius of such "effective" spurs were found to be about 5 nm for four pairs or 9–10 nm for five pairs.

Keywords: Radical ion pair; Nonpolar solution; Delayed fluorescence; Radiation track structure; Time-resolved magnetic field effect; Time-resolved electric field effect

1. Introduction

The analysis of irradiation-induced reactions in the track of an ionizing particle is known to be complicated by, firstly, quite a variety of possible reactions and, secondly, the complexity of the kinetic law of these reactions due to nonhomogeneous spatial distribution of active species. These circumstances necessitate the use of computer modeling for studying the early stages of radiolysis. At present, the most adequate approach to develop such a model is likely to be the computer simulation of the movement of ions and other active species in the track, starting from an initial spatial distribution of thermalized primary charge carriers (Schmidt, 1983; Lozovoy et al., 1990; Sauer et al., 1991; Bartczak and Hummel, 1997; Anishchik et al., 1998).

Recently, a model of this kind was suggested to describe the yield of electronically excited species in irradiated alkane solutions as well as the effect of electric and magnetic field on the kinetics of delayed fluorescence (Borovkov and Velizhanin, 2006). In that work an attempt was made to take into consideration all factors, which were conventionally believed to be responsible for excited states formation. The reaction scheme compiled, besides ion pair recombination, reaction of electronic excitation energy transfer, triplet–triplet annihilation as well as excited state quenching due to contact interactions involving the intermediates in irradiated alkane solution.

The present work describes the application of this computer model to the analysis of experimental delayed fluorescence decays measured in the range 0–250 ns after X-ray pulsed irradiation of *n*-dodecane solutions of *N,N,N′,N′*-tetramethyl-*para*-phenylenediamine (TMPD). Furthermore, the effect of external magnetic and electric fields on these decays is also discussed. The system was chosen for the analysis because of its relative simplicity. Primary radical cations of *n*-dodecane are comparatively stable species, and their mobility is close to the mobility of molecular ions (Saeki et al., 2001; Borovkov et al., 2002). TMPD molecules capture solvent holes due to their low ionization potential of 6.2 eV (Kondratyev, 1974) but do not capture excess electrons. The low mobility of excess electrons in dodecane makes it possible to register the

---

[*] Corresponding author. Institute of Chemical Kinetics and Combustion, SB RAS, Novosibirsk 630090, Russian Federation.
Fax: +7 3833 307 350.
E-mail address: borovkov@kinetics.nsc.ru (V.I. Borovkov).

0969-806X/$ - see front matter © 2006 Elsevier Ltd. All rights reserved.
doi:10.1016/j.radphyschem.2006.09.007

recombination kinetics of ($TMPD^{+\bullet}/e^-$) pairs in nanosecond time domain (Borovkov et al., 1997).

This work also addresses the question what an "effective" spur is in irradiated alkanes. Such "effective" spur is thought to be the simplest one, which allows describing as many as possible experimental facts including manifestations of intermediates interactions without considering full-scale track structure. In the present work, the initial spatial distribution of solvent holes and excess electrons in "effective" spur in *n*-dodecane irradiated by 20-keV X-ray quanta is determined relying on reproducing the yields of both free ions and singlet excitations as known from literature as well as kinetic dependences reported here for the first time. Such single-spur model is the successive stage as compared to the single-pair model (Hummel, 1987) to include reactions between short-lived intermediates in irradiated solution.

According to the results of Borovkov and Velizhanin (2006), the geometric parameters of an "effective" spur can be determined in a more correct manner by a combined analysis of the effects of external electric and magnetic fields on the fluorescence kinetics. This is because electric field is a natural tool to separate the contribution of ion pair recombination to the intensity of delayed fluorescence from other ones. In turn, the effect of magnetic field is determined largely by the fraction of geminate radical ion pairs, i.e., by the geometrical structure of the spur (Anishchik et al., 1998).

2. Experimental

Delayed fluorescence of *n*-dodecane solutions under ionizing irradiation was detected by the single photon counting technique using an X-ray fluorimeter described elsewhere (Anishchik et al., 1989). The duration of the ionizing pulse was about 2 ns with quantum energy of about 20 keV. The collected light was passed through an optical bandpass filter (380–480 nm). The sample cuvette design allowed measuring the influence of applied electric field on the fluorescence intensity and was similar to that described elsewhere (Borovkov et al., 1997). The studied solution was flooded into the space between parallel electrodes placed with the gap of 2.3 ± 0.07 mm. The solution was irradiated through the thin wall of one of the electrodes. Fluorescence was detected in perpendicular direction relative to irradiation. All of the parts of the cuvette were made of nonferromagnetic materials and measuring of magnetic field effects was performed in the same experimental conditions as for the electric field effects.

To quantitatively analyze the effects of the external fields, the ratios $I_{E,B}(t)/I_0(t)$ were used, where $I_{E,B}(t)$ and $I_0(t)$ were kinetics of delayed fluorescence registered with electric (E) or magnetic (B) field applied to the irradiated solution and kinetics without the external fields, respectively. These ratios are referred to as time-resolved electric field effects (TR EFE) and magnetic field effects (TR MFE), respectively (Borovkov et al., 1995, 1997, 2003; Klein and Voltz, 1977; Veselov et al., 1991; Brocklehurst, 1997; Bagryansky et al., 2004). To reduce the influence of instrumental drift, the fluorescence decays were recorded for periods of 250 s, alternatively, with and without external fields. The electric field strength in solution was up to 24 kV/cm with an accuracy of about ±5%. The nonzero magnetic field was equal to 0.1 T. Zero magnetic field was adjusted to within ±0.05 mT.

The rate constant of triplet–triplet annihilation of triplet-excited TMPD molecules in liquid dodecane was measured using a conventional laser flash-photolysis setup (excimer XeCl laser, 308 nm, 15 ns, 30 mJ) described in detail in Grivin et al. (1990). The measurement procedure for the rate constant was very similar to the one described in Okamoto et al. (2001). Briefly, the absorption by $^3TMPD^*$ was measured at different intensities of the excitation laser pulse and the rate constant of $^3TMPD^*$ absorption decay in bimolecular process was determined. The obtained absorption characteristics for $^3TMPD^*$ ($\lambda_{max} \approx 600$ nm, $\varepsilon \approx 1.2 \times 10^4$) were close to the literature values (Potashnik et al., 1969; Carmichael and Hug, 1986). Laser pulse power was controlled by a Fieldmaster power/energy meter (Coherent, Inc.). Optical density of the sample (1 cm) in the series of the experiments was varied from 0.1 to 0.4.

n-Dodecane (Fluka, 99%) was stirred with concentrated sulfuric acid, washed with water, passed several times through a 1 m column of activated alumina, and stored over sodium. Using gas chromatography, we found that the used *n*-dodecane contained several methylundecanes (about 1%) as the main impurities. Other impurities were found to amount to about 0.1% and were not identified. Dodecane isomers could not be removed from the solvent by the purification procedure, but their presence is believed to have no significant effect on the obtained results. TMPD (Aldrich, 99%) was sublimed under vacuum several times before use. Hexafluorobenzene (HFB, 99%), 1-bromohexane (98%), and diphenylacetylene (DPA, 98%) were used as received from Aldrich. The solutions were degassed by repeated freeze-pump-thaw cycles. All measurements were performed at 293 ± 0.5 K.

3. Description of the model and choice of the parameters

3.1. Outline of the algorithm

The algorithm for modeling the processes initiated by irradiation and the used reaction scheme are described in detail by Borovkov and Velizhanin (2006). In this section, we give a basic sketch of the model. This simulates the radiation-induced reactions starting from an isolated spherical spur, because in order to simulate the early steps of the radiolysis it is sufficient to consider only species born close to each other. The active species, whose reactions were considered and, consequently, whose coordinates and states were processed in the program, were excess electrons, (e^-), dodecane and TMPD radical cations ($S^{+\bullet}$, $D^{+\bullet}$), singlet and triplet excited dodecane and TMPD molecules ($^{1,3}S^*$, $^{1,3}D^*$). It was assumed that $^3S^*$ decayed instantly forming a pair of neutral radicals $^3(R^\bullet \ldots R^\bullet)$ (Brocklehurst, 1992a, b; LaVerne et al., 1997). Parameters of all these intermediates are given in Table 1. For brevity, Table 2 lists only the main reactions that, in the framework of the used model, contribute substantially to the delayed fluorescence intensity and to external field effects. The only reaction between the active intermediates included in Table 1 is the annihilation of triplet TMPD molecules ($^3D^*$). Other possible encounter reactions of the intermediates can be found in Borovkov and Velizhanin (2006). In Table 2 also given are the values of rate constants as well as effective radii and probabilities for the reactions.

The modeling of the motion and reactions of the intermediates starts from a random placing a number of solvent radical cations in a spherically shaped spur, and placing excess electrons isotropically distributed around corresponding cations to form ion pairs. Then diffusion displacement of the species and the drift of the charged species in the electric field of the surrounding ions and the external electric field, if the latter was non-zero, were calculated. At each step of the program, the probabilities of quasi-monomolecular reactions for the species were calculated. Reactions between active species were considered to occur if the distance between the species became smaller than the sum of their radii. Reactions with a neutral TMPD molecule were described as a quasi-monomolecular reaction with a rate constant $k(t) = 4\pi R_0 D_0(1+R_0/(\pi D_0 t)^{1/2})$, where R_0 is reaction radius and D_0 is the sum of the diffusion coefficients of the reagents. In Table 2, $4\pi R_0 D_0$ values are given as rate constants.

The program produced a file where the moments of all the events processed by the algorithm were recorded. These were the recombination of oppositely charged species, formation of neutral radicals or excited states of various multiplicities, radiative deactivation of singlet excited states, as well as encounters of all active species. For recombination of radical ion pairs, it was also taken into account whether the radical ions were born as one pair (geminate recombination) or not (cross recombination).

Table 1
Characteristics of particles involved in reactions (1–11)[a]

Particle	D (cm^2/s)	μ (cm^2/Vs)	R (nm)[c]	$T_2 = T_0$ (ns)	T_1 (ns)
$C_{12}H_{26}^{+\bullet}$	6.5×10^{-6}	2.6×10^{-4b}	0.5	30 ± 10^b	200 ± 50^b
e^-	2.1×10^{-4}	8.5×10^{-3b}	0.5	∞	∞
TMPD$^{+\bullet}$	3.8×10^{-6}	1.5×10^{-4b}	0.38	$(k_{11c})^{-1d}$	220 ± 50^b
$C_{12}H_{26}^*$	8.9×10^{-6c}	—	0.5	—	—
TMPD (TMPD*)	8.2×10^{-6c}	—	0.38	—	—
$R^\bullet$	8×10^{-6c}	—	0.4	—	—

[a] D is the diffusion coefficient, μ is the mobility, R is particle's radius, T_1, T_2, and T_0, are the times of spin-lattice relaxation, phase relaxation in strong magnetic field and in zero field, respectively.

[b] As determined in this work.

[c] Estimated as described in the text.

[d] Relaxation rate depends on TMPD concentration (see text and Appendix A.1).

3.2. Model parameters

The most part of the model parameters used to fit the experiment were determined by supplementary measurements or by estimation from data available in literature (vide infra). However, some of them were obtained as a result of the search of optimal accordance between the experiment and the simulation.

First of all, parameters concerned with the spatial distribution of primary ion pairs in the spur were varied to reach the accordance. These were the spur radius, the initial number of ion pairs, and the distribution function of the initial distances between geminate ions. Spur radius value and the number of ion pairs were varied between 1 and 20 nm and between 2 and 10 pairs, respectively. Distribution function of the primary ion-electron ($S^{+\bullet}/e^-$) pairs was chosen in the exponential form $f(r>a) = 1/b \exp(-(r-a)/b)$, where $a = 1$ nm was the closest distance between approaching oppositely charged species. Parameter b was selected so as to obtain the free ion yield in electric fields of 0 and 10 kV/cm were about 2.2% and 3.5% of initial number of ions, respectively. These values came from the premise that four ion pairs arose per each 100 eV of absorbed energy, and the yield of free ions in *n*-dodecane irradiated with 20 keV X-rays was equal to yield in *n*-hexane in similar conditions and amounted to 0.09/100 eV (Schmidt and Allen, 1970; Holroyd and Sham, 1985). Changing the distribution function to $f(r>a) \sim \exp(-(r-a)^2/b^2)$ gave somewhat worse results.

The better and approximately equivalent descriptions of experiment were obtained using spurs of 5–5.5 nm in radius containing initially four ion pairs or spurs of 9–10 nm in radius containing five ion pairs, with $b = 4.2$–4.5 nm. The calculated curves given below, unless indicated otherwise, were calculated for the case of four pairs in spur of 5 nm in radius with $b = 4.3$ nm.

An additional criterion for choosing the spur structure was the probability of geminate recombination of $S^{+\bullet}/e^-$ pairs, which for the majority of such pairs occurs in sub-nanosecond time domain. Therefore, the spin state of these geminate pairs is singlet, and their fraction determines the yield of singlet excited solvent molecules. According to Holroyd et al. (1997), the yields of singlet-excited molecules of *cis*- and *trans*-decalin for energy of irradiation quanta 15 keV are about 1.9 and 2.5 excitations per 100 eV. For dodecane, the corresponding value was taken to be equal to about two, so the probability of geminate recombination should be about 0.5. This value is also validated by the results obtained by Sauer and Jonah (1994). All the presented results of modeling match up to this criterion.

Other adjustable parameters were the rate constant of the energy transfer reaction (6) and the yield of ^{1}TMPD* in

Table 2
Rate constants, radii and probabilities of the most important reactions used in simulation[a]

Reaction		Rate constant	Reaction radius (nm); (reaction probability)
$S \rightarrow S^{+\bullet} + e^-$	(1)	—	—
$S^{+\bullet} + e^- \rightarrow {}^{1,3}S^*$	(2)	—	1; (1)
$S^{+\bullet} + D \rightarrow S + D^{+\bullet}$	(3)	$(9.8 \pm 0.7) \times 10^{9}\,M^{-1}\,s^{-1}$[b]	0.88 ± 0.1[b]; (1)
$D^{+\bullet} + e^- \rightarrow {}^{1,3}D^*$	(4)	—	1; (1)
${}^{1}S^* \rightarrow {}^{3}S^*$	(5)	$2.4 \times 10^{8}\,s^{-1}$	—
${}^{1}S^* + D \rightarrow S + {}^{1}D^*$	(6)	$(1.1 \pm 0.3) \times 10^{10}\,M^{-1}s^{-1}$[b,c]	0.88 ± 0.3[b]; (0.45)
${}^{1}S^* + D \rightarrow S + {}^{3}D^*$	(6′)	—	0.88 ± 0.3[b]; (0.55)
${}^{1}D^* \rightarrow {}^{3}D^*$	(7)	$1.9 \times 10^{8}\,s^{-1}$	—
${}^{3}D^* + {}^{3}D^* \rightarrow D + {}^{1}D^*$	(8)	$(9.4 \pm 0.4) \times 10^{9}\,s^{-1}$[b,c]	0.76 ± 0.2; (1/9)
${}^{3}D^* + {}^{3}D^* \rightarrow D + {}^{3}D^*$	(8′)	—	0.76 ± 0.2; (1/3)
${}^{1}D^* \rightarrow D + h\nu$	(9)	$1.8 \times 10^{7}\,s^{-1}$	—
$S^{+\bullet} + (S)' \rightarrow S + (S^{+\bullet})'$	(10)	$10^{8}\,s^{-1}$	—
$D^{+\bullet} + (D)' \rightarrow D + (D^{+\bullet})'$	(11)	$(5 \pm 1.5) \times 10^{9}\,M^{-1}\,s^{-1}$[b]	—

The complete collection of the reactions used can be found in ref. (Borovkov and Velizhanin, 2006).

[a] Here S is the solvent molecule, e^- is the excess electron, D is the TMPD molecule, S^* and D^* are the molecules in excited states with their multiplicity indicated.

[b] As determined in this work.

[c] For the values of rate constants the values of $k = 4\pi R_0 D_0$ are given.

this reaction. To obtain a satisfactory agreement between the experiment and the simulation within the initial portion (0–50 ns) of the decays at TMPD concentration ranged from 1 to 20 mM the value $1.1 \times 10^{10}\,M^{-1}/s$ for encounter frequency of the reactants in reaction (6) was chosen. Note this is comparable with a value of $1.7 \times 10^{10}\,M^{-1}/s$ reported earlier for the rate constant of the diffusion-controlled reaction of energy transfer from excited *n*-dodecane molecules to benzene (Mehnert et al., 1988). Besides, to provide, in parallel with the agreement of the earlier portions of the fluorescence decays, the proper contribution of triplet–triplet annihilation at longer time, the probability of the formation of a singlet excited molecule ${}^{1}TMPD^*$ in the reaction (6) was taken equal to 0.45 ± 0.05, assuming the formation of ${}^{3}TMPD^*$ in the rest of the cases (reaction (6′)).

3.3. Diffusion coefficients of the reactive particles

Diffusion coefficients D of the neutral species were determined using data reported in Blum et al. (1985), Kowert et al. (2001), and Kowert et al. (2003), where empirical dependencies of the diffusion coefficients of aromatic molecules on molecule size and solvent viscosity, as well as self-diffusion coefficients of *n*-alkanes, are given. According to Kowert et al. (2001), in *n*-dodecane at 293 K the diffusion coefficient of DPA molecules, which have similar volume and shape to molecules of TMPD, is about $8.2 \times 10^{-6}\,cm^2/s$. This value was used for neutral TMPD molecules. For the diffusion coefficient of solvent molecules the value of $8.9 \times 10^{-6}\,cm^2/s$ was taken, which was obtained from averaging the values published in Blum et al. (1985) and Kowert et al. (2003) for 25 °C under the assumption that the coefficient is proportional to solvent viscosity raised to the power 0.8. Such dependence corresponds to the case of solute and solvent molecules with approximately equal sizes. The diffusion coefficients of a molecule in its electronically excited and ground states were taken to be the same (Terazima, 2000; Ukai et al., 2000).

Diffusion coefficients of charge carriers involved were determined using Nernst–Einstein relationship $\mu/e = D/kT$ from the mobilities of the species measured by the method of TR EFE, which allows determining the sum of mobilities of the recombining radical ions (Borovkov et al., 2003).

The mobility of excess electrons ($8.5 \times 10^{-3}\,\mathrm{cm^2/Vs}$ at 293 K) was determined from TR EFE curves for *n*-dodecane solutions of TMPD. In this case, the observed mobility was provided almost exclusively by electron movement. In order to measure the mobility of radical cations, experimental conditions should be chosen in such a way that the radical ion pair would include a slow radical anion with a known mobility.

A suitable electron acceptor is HFB, which captures only excess electrons in dodecane solutions. The mobility of $\mathrm{HFB}^{-\bullet}$ ($2.4 \times 10^{-4}\,\mathrm{cm^2/Vs}$) was measured using approach exploited before in Borovkov et al. (2003) for a similar measurement in *n*-hexane. Briefly, the relative mobility of the secondary radical ions $\mathrm{DPA}^{+\bullet}$ and $\mathrm{HFB}^{-\bullet}$ in *n*-dodecane solution of 3 mM HFB + 3 mM DPA was measured. Then this relative mobility value was decreased by that for DPA radical cation in *n*-dodecane ($1.6 \times 10^{-4}\,\mathrm{cm^2/Vs}$), which was determined earlier (Borovkov et al., 2003).

The mobility value ($2.6 \times 10^{-4}\,\mathrm{cm^2/Vs}$) of the solvent hole (or the corresponding alkene radical cation, a possible product of the decay of a primary radical cation), was calculated as the difference between the relative mobility of radical ions in *n*-dodecane solution of 10 mM HFB and the mobility of $\mathrm{HFB}^{-\bullet}$. The mobility of $\mathrm{TMPD}^{+\bullet}$ ($1.5 \times 10^{-4}\,\mathrm{cm^2/Vs}$) was determined using dodecane solution of 3 mM TMPD + 3 mM DPA, in which the positive charges rest on the TMPD molecules and the negative charges are on DPA molecules. Note that diffusion coefficient of TMPD molecule is twice as much as that of $\mathrm{TMPD}^{+\bullet}$. This is in accordance with the results reported earlier (Terazima et al., 1995).

Diffusion coefficients of neutral radicals were selected arbitrarily. The value of this parameter is of no importance because the contribution of neutral radicals in the discussed processes is insignificant (Borovkov and Velizhanin, 2006). All diffusion coefficient values used in the simulation are summarized in Table 1.

3.4. Rate constants for reaction of secondary radical cation formation

In order to determine the rate constant k_3 of the formation of $\mathrm{D}^{+\bullet}$ in reaction (3) an approach suggested in Borovkov and Velizhanin (2004) was used. In this, like to the methods of TR EFE or TR MFE, the relative change in the fluorescence decay of solutions of 10 mM HFB caused by the addition of a certain amount of TMPD was analyzed. According to the results of the cited work, the ratio between the fluorescence decay for the solution, which contains both HFB and TMPD, and that containing only HFB, gives the kinetics of $\mathrm{TMPD}^{+\bullet}$ formation via reaction (3). The rate constant of reaction (3) averaged over a series of measurements with different TMPD concentrations was found to be $(9.8 \pm 0.7) \times 10^9\,\mathrm{M^{-1}/s}$.

3.5. Rate constants for reaction of triplet–triplet annihilation

As was mentioned above the measurement procedure for the rate constant of the triplet TMPD molecule decay in reaction (8) was close to the one described in Okamoto et al. (2001). Lifetime of $^3\mathrm{TMPD}^*$ in quasifirst order reaction was found to be about 50 µs. The second order rate constant k_{TTA} of $^3\mathrm{TMPD}^*$ decay via reaction

$$2\,{}^3\mathrm{D}^* \rightarrow {}^1\mathrm{D}$$

was obtained to be $2k_{\mathrm{TTA}} = (4.3 \pm 0.2) \times 10^9\,\mathrm{M^{-1}/s}$. In order to estimate the frequency of encounters between $^3\mathrm{TMPD}^*$ it was assumed that the process of triplet–triplet annihilation (TTA) involving $^3\mathrm{TMPD}^*$in dodecane solution of TMPD is described by the same reaction scheme (Scheme 1) as for *n*-hexane and methylcyclohexane solutions of 2-acetonaphthone studied in Okamoto et al. (2001). Here D denotes TMPD molecule.

According to the results of the mentioned work (Okamoto et al., 2001), the constant k_{TTA} can be expressed in the following way

$$\frac{1}{2k_{\mathrm{TTA}}} = \frac{1}{k_{\mathrm{diff}}}\frac{k_{\mathrm{S}} + k_{\mathrm{T}} + k_{-\mathrm{diff}}}{k_{\mathrm{T}} + (1+\varphi)k_{\mathrm{S}}}.$$

Here k_{diff} and $k_{-\mathrm{diff}}$ are diffusion rate constants of the formation and the decay of an encounter complex of triplet molecules, respectively, k_{T} is the rate constant of reaction $({}^3\mathrm{D}^*)_2 \rightarrow {}^3\mathrm{D}^* + \mathrm{D}$ proceeding in the complex, k_{S} is the rate constant of the parallel reaction $({}^3\mathrm{D}^*)_2 \rightarrow {}^1\mathrm{D}^* + \mathrm{D}$, φ is the fluorescence quantum yield of $^1\mathrm{D}^*$. In this work, the value $\varphi = 0.09$ (Nakamura et al., 1984) was used, and it was assumed that there were no channels of $^1\mathrm{D}^*$ deactivation other than intercombinational conversion.

Unfortunately, because of the nonlinearity of the photomultiplier tube used in laser flash photolysis experiments, we could not determine the ratio between the intensity of fluorescence of directly excited singlet TMPD molecules (at $t < 50$ ns) and the intensity coming from triplet–triplet annihilation with sufficient accuracy. In other words, we could not get information about the $k_{\mathrm{S}}/k_{\mathrm{T}}$ ratio from an independent experiment. Therefore, it was assumed that the rate constants $k_{-\mathrm{diff}} \gg k_{\mathrm{diff}}$ and $k_{\mathrm{S}}{:}k_{\mathrm{T}}{:}k_{-\mathrm{diff}} = 1{:}3{:}5$. In other words, the state of triplet molecules in a quintet complex does not change and the outcome of encounter between two triplet TMPD molecules is completely determined by the multiplicity of the initial pair of triplets. Under these assumptions, the probabilities of forming $^1\mathrm{TMPD}^*$ and $^3\mathrm{TMPD}^*$ in

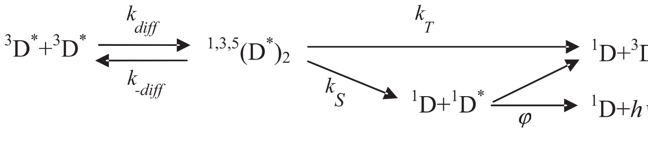

Scheme 1.

reaction (8) are 1/9 and 1/3, respectively, and $k_{\mathrm{diff}} = (9.4 \pm 0.4) \times 10^9\,\mathrm{M}^{-1}/\mathrm{s}$ (Table 2). These data were used to describe accurately reaction (8) and to estimate characteristic radius of $^3\mathrm{TMPD}^*$ (vide infra).

3.6. Sizes of particles

According to results of the work by Bondi (1964), if TMPD molecule is considered to be a ball then its radius is about 0.29 nm. For *n*-dodecane, such an estimate looks too crude. As a characteristic geometric size of this particle the value $(R_x R_y R_z)^{1/3} \approx 0.38\,\mathrm{nm}$ can be taken, where R_i is the dimension along the corresponding axis estimated from bond lengths and atomic radii in the molecule of dodecane.

However, it is well known that the average distance at which a diffusion-controlled reaction occurs can substantially differ from the sum of van-der-Waals radii of the reagents (Doktorov and Burstein, 1975; Heisel and Miehe, 1982). The effective reaction radius for a reaction with rate constant k is determined as $R_\mathrm{e} = k/4\pi D$, where D is the sum of diffusion coefficients of the two reagents. Using the rate constants for processes discussed above one can calculate that effective radius of reaction (3) of electron transfer from a TMPD molecule to a radical cation of dodecane is about 0.88 nm, contact radii for $^3\mathrm{TMPD}^*$ triplet–triplet annihilation is about 0.76 nm and that for energy transfer reaction (6) is about 0.88 nm.

When estimating the effective radius of electron transfer in the reaction of electron self-exchange (11) it should be remembered that the rate constant of this reaction $5 \times 10^9\,\mathrm{M}^{-1}/\mathrm{s}$ (Table 2) is determined indirectly, from concentration dependence of phase relaxation rate for radical ion pairs. For sufficiently high rate of electron transfer, the probability that the unpaired electron would remain at the original partner in the same magnetic environment is 0.5. If the duration of contact is much shorter than the characteristic time of singlet–triplet transitions $1/\gamma\sigma \approx 4\,\mathrm{ns}$, the exchange rate is only half the rate of binary encounters of reagents in reaction (11). Here $\sigma = 1.43\,\mathrm{mT}$ is ESR spectrum width for radical cation $\mathrm{TMPD}^{+\bullet}$ (Fisher, 1990), γ is gyromagnetic ratio for electron. The effective radius of electron transfer in reaction (11) estimated by this way is $R_\mathrm{e} \approx 1.1\,\mathrm{nm}$, which exceeds doubly the sum of "geometric" dimensions of reagents. On the other hand, if the duration of contact is large enough that each encounter effectively contributes to the rate of phase relaxation, electron transfer radius in reaction (11) should be reduced to one-half of the above estimate.

As a summary, in this work the following radii were taken when considering binary encounters: 0.38 nm for effective size of excited and ionized TMPD molecules, 0.5 nm for dodecane molecules, 0.4 nm for neutral radicals, 0.5 nm for excess electrons. The particular size attributed to excess electron is not very significant, since in nonpolar solutions the reaction of ion neutralization, where electron participates, only weakly depends of the reagent radii. In addition, collisions of electrons with neutral particles have not very significant effect on the yield of excited states at the ionization densities considered in this study (Borovkov and Velizhanin, 2006).

3.7. Lifetimes of excited states

Lifetime of isolated singlet excited solvent molecule $^1\mathrm{S}^*$ was taken to be 4.2 ns as determined in experiments with photoexcitation of dodecane (Shinsaka et al., 1985). In Table 2 the inverse of the $^1\mathrm{S}^*$ lifetime is given as rate constant of reaction (5), since quantum yield of fluorescence for dodecane molecules is negligibly low (Rothman et al., 1973).

The lifetime and the quantum yield of $^1\mathrm{TMPD}^*$ were taken to be $\tau_{\mathrm{fl}} = 4.9\,\mathrm{ns}$ and $\varphi = 0.09$, respectively (Nakamura et al., 1984). The value of $\tau_{\mathrm{fl}} = 4.3\,\mathrm{ns}$ as measured in isooctane solutions is also given in Schmidt et al. (1990), but the experimental kinetics cannot be satisfactorily described using such short value. Quite the contrary, modeling shows that somewhat better results are obtained assuming $\tau_{\mathrm{fl}} = 5\,\mathrm{ns}$.

In Table 2 the values $k_7 = (1-\varphi)/\tau_{\mathrm{fl}}$ and $k_9 = \varphi/\tau_{\mathrm{fl}}$ are given as the rate constants for reactions (7) and (9), respectively. A possible uncertainty in the magnitude of φ has an insignificant effect on the results of modeling, as every component of the fluorescence kinetics gives a contribution proportional to φ. As long as $\varphi \ll 1$, such an uncertainty will have only very weak effect on the contribution of triplet–triplet annihilation.

3.8. Spin dynamics of geminate radical ion pairs

Determination of the probability of singlet-excited luminophore yield upon recombination of radical ion pairs requires taking into consideration spin dynamics of geminate radical ion pairs, i.e. the probability of finding such a pair in its singlet state at the moment of recombination $\rho_{\mathrm{ss}}(t)$ (see Appendix A).

Experimental curves of TR MFE as presented in this work did not show pronounced quantum beats, and comparison with experiment was performed using the level of magnetic field effect at times comparable or exceeding phase relaxation times. So to reduce computational costs of simulations a simplified way of TR MFE curve calculation was employed. As it was in Borovkov and Velizhanin (2006), when calculating spur reactions it was assumed that the probability of producing a singlet excitation in the recombination of geminate pairs $\mathrm{S}^{+\bullet}/e^-$ is equal to 1, and in the recombination of geminate pairs $\mathrm{D}^{+\bullet}/e^-$ this probability is equal to 0.25. This assumption is likely to be valid for the TMPD solutions because of rather high rate of singlet–triplet transitions due to phase relaxation time and hyperfine interactions in radical cations.

The explicit details of spin dynamics were accounted for only when calculated TR MFE curves were compared with the experimental ones. Paramagnetic relaxation time of $S^{+\bullet}$ and $TMPD^{+\bullet}$ as well as the rate constant of the electron self-exchange of $TMPD^{+\bullet}$ in reaction (11) were determined from the modeling of magnetic field effects. Details of these TR MFE curves calculation for zero and nonzero magnetic field are presented in Appendix A. The simplified procedure of TR MFE calculations leads only to minor deviations in the yield of triplet TMPD molecules and in the contribution of TTA in the total intensity of fluorescence. Since about 90% of $^1TMPD^*$ are converted to triplets, such a simplification results in the change of $^3TMPD^*$ yield not greater than few percents. Trial calculations with explicit account of spin dynamics during the radical ion pair recombination in the spur have demonstrated that within stochastic deviations the calculated fluorescence decays and TR MFE curves were not distorted by this simplification.

In calculation of spin dynamics, it was taken into account that radical cations of dodecane and TMPD took part in the reactions of electron self-exchange (Grampp and Jaenicke, 1984; Werst, 1996; Borovkov et al., 2002), which have no effect on the mobility of charges and show up in spin dynamics only as phase relaxation:

$$S^{+\bullet} + S' \rightarrow S + (S')^{+\bullet} \quad \text{(reaction 10 in Table 2)},$$

$$D^{+\bullet} + D' \rightarrow D + (D')^{+\bullet} \quad \text{(reaction 11 in Table 2)}.$$

In the model, we did not consider the possibility of transforming the primary solvent radical cation into a corresponding olefinic radical cation (Schwarz et al., 1981; Werst et al., 1990). Such decomposition has practically no effect on the mobility of this charge carrier and does not change significantly the rate of TMPD radical cation formation. It is clear that the formation of olefinic radical cation having ESR spectrum width substantially larger than the width of $S^{+\bullet}$ would affect spin dynamics of radical ion pairs. However, in the conditions of limited experimental accuracy this effect can be adequately taken into account by an additional shortening of phase relaxation time (Borovkov et al., 2002).

4. Results and discussion

4.1. Key components of delayed fluorescence decay (qualitative analysis)

This section qualitatively describes some features of the delayed fluorescence decays initiated by pulsed irradiation of TMPD solutions in dodecane. Additionally, here the effects of electric field and electron acceptors are discussed in short. Figs. 1a and 1b show experimental decays registered in the case of solutions of 20 mM (a) and 1 mM (b) TMPD concentration, as well as these decays after applying external electric field, adding electron acceptor (0.3 mM of 1-bromohexane), or saturating the solution with atmospheric air.

Fig. 1a shows that application of electric field and addition of 1-bromohexane lead to very similar transformations of the observed fluorescence kinetics. Both the factors suppress the $TMPD^{+\bullet}/e^-$ pairs contribution to the fluorescence intensity at rather long times. Electric field rapidly decreases the recombination probability for pairs $TMPD^{+\bullet}/e^-$ (Borovkov et al., 1997). Excess electron capture by bromohexane, which in *n*-dodecane proceeds with rate constant about $10^{11}\,M^{-1}/s$ via dissociative electron attachment, suppresses the formation of $TMPD^*$ upon recombination of the ion pair formed after the capture (Werst, 1996; Borovkov and Velizhanin, 2004). A several-fold increase in the concentration of bromohexane results in a further decrease of fluorescence intensity in the time range 50–250 ns, but addition of bromohexane has a weaker effect than addition of air oxygen, which is not

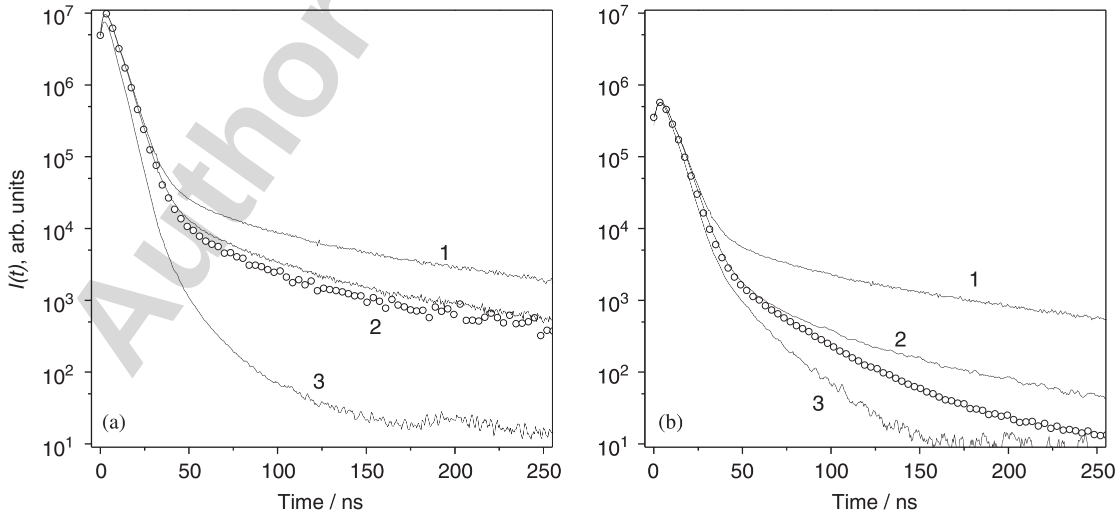

Fig. 1. Experimental delayed fluorescence decay curves of 20 mM (a) and 1 mM (b) TMPD solutions in *n*-dodecane (curves 1 in both parts), as well as the decay curves for the same solutions upon application of external electric field of 24 kV/cm (curves 2), upon addition of 0.3 mM 1-bromohexane (circles), and upon saturation of the solution with atmospheric air (curves 3).

only an electron acceptor, but also a quencher of molecular excited states (Lissi and Encinas, 1989). The main difference for the solution with lower concentration of TMPD (Fig. 1b) is a significantly stronger effect of both application of electric field and addition of bromohexane.

Therefore, in the solution of 20 mM TMPD in dodecane a substantial contribution to fluorescence intensity is due to ^{1}TMPD* formation in a channel, which is not originated from electron recombination. A comparison with the results of computer simulation of spur recombination (Borovkov and Velizhanin, 2006) leads to the conclusion that at times shorter than 50 ns the fluorescence is dominated by the processes of energy transfer from excited solvent molecules to TMPD. In turn, at times longer than 50 ns the substantial contribution to fluorescence intensity is due to triplet–triplet annihilation (TTA) of ^{3}TMPD*.

4.2. *Comparison of experimental fluorescence decay curves with simulation results*

Fig. 2 shows the ultimate agreement between calculated and experimental kinetics of delayed fluorescence at various concentrations of TMPD. The calculated curves were obtained with values of parameters given in Tables 1 and 2 for spur with radius of 5 nm initially containing four ion pairs. The presented curves correspond to equal absorbed doses or numbers of simulation cycles.

Note that the shape of the geminate recombination kinetics only weakly depends on the mobility of the recombining charges and spur structure (Borovkov and Velizhanin, 2006), and the demonstrated accordance between the experimental and the simulated fluorescence kinetics could be attained using very different values for parameters of the model. The most definite conclusions that may be drawn from the fluorescence decay shape concerns the relative contribution of energy transfer processes and to the occurrence of reactions leading to an abrupt change in the yield of excited states upon recombination of ion pairs. That is why the use of the external fields to probe the fluorescence decays is sure to be essential for the examination of primary radiation-induced processes.

4.3. *Time-resolved electric effect*

Fig. 3 shows experimental (solid lines) and calculated (scatter plots) TR EFE curves for solutions with different concentration of TMPD. The best agreement with the experiment was achieved with electron mobility of 0.0085 cm^2/Vs, which is substantially lower than the earlier reported values of 0.0038 cm^2/Vs (Schmidt, 1977) and 0.02 cm^2/Vs (Gee and Freeman, 1987). A possible reason for such a discrepancy is the presence of impurities with negative electron affinities, which within a very short time capture the electron thus lowering its apparent mobility (Schmidt, 1997; Holroyd and Nishikawa, 2002). As an additional indication for this, a somewhat higher value of

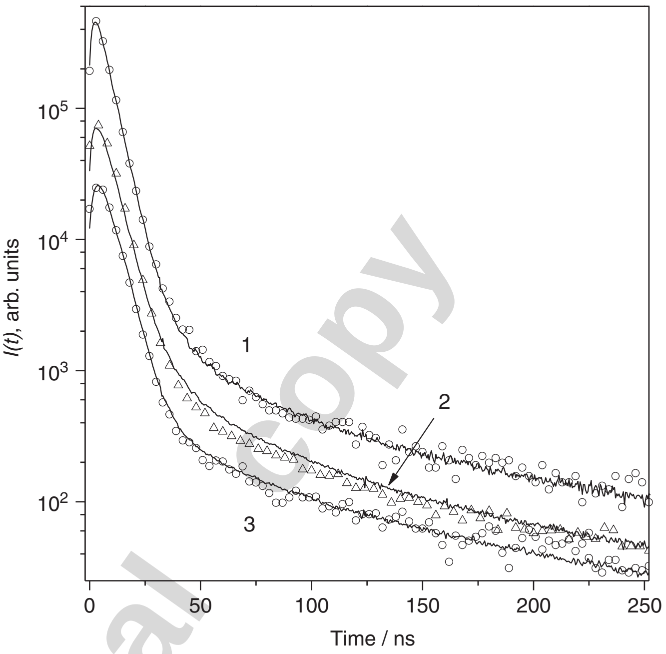

Fig. 2. Experimental (lines) and calculated (circles) decay curves of delayed fluorescence from solutions of 20 mM (curves 1), 3 mM (curves 2) and 1 mM (curves 3) TMPD in *n*-dodecane. The calculated curves were obtained for parameter values given in Tables 1 and 2, for spur with radius of 5 nm initially containing four ion pairs. All experimental curves are normalized to equal absorbed dose, and all calculated curves were obtained using the same number of computation cycles (10^6).

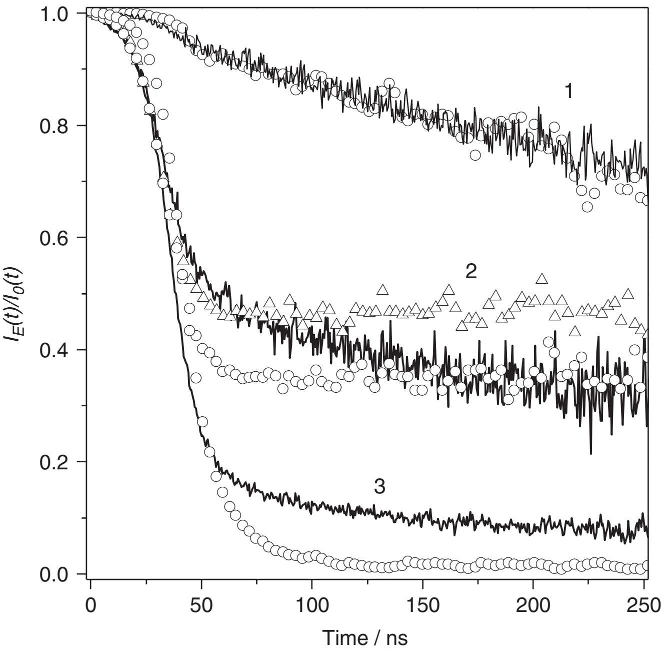

Fig. 3. Experimental (lines) and calculated (symbols) curves of time-resolved electric field effect for TMPD solutions in dodecane. All calculated curves except for the one as shown with (triangles) were obtained for spur of 5 nm in radius with four pairs. Curves (1): TMPD concentration is 1 mM, electric field strength is $E = 4$ kV/cm. Curves (2): TMPD concentration is 20 mM, $E = 24$ kV/cm, with triangles the calculated curve for five pair in spur of 9 nm in radius is shown. Curves (3) TMPD concentration is 1 mM, $E = 24$ κV/cm. Parameters of the modeling are given in Tables 1 and 2.

the activation energy for electron mobility in the used dodecane—0.24 eV instead of 0.2 eV reported by Schmidt (1977) could be considered.

In the field of 24 kV/cm a delay in the quenching of fluorescence is observed, which is connected with the weak dependence of reactions (6) and (9) on the applied electric field. As is readily seen from Fig. 3, complete quenching is not achieved even at times $t > 100$ ns and the curves reach a plateau with level depending on TMPD concentration. In full accordance with the above qualitative consideration, the simulation demonstrates that incomplete quenching in the more concentrated solution can be almost exclusively attributed to contribution of TTA reaction. However, the simulation fails to reproduce a slight increase in the degree of quenching by the field, which is observed in experiment. Probably an unaccounted process leading to additional decay of ^{3}TMPD*is present in the real solution.

The calculated curves for the solution of 20 mM TMPD are presented in two versions, for four pairs in spur of 5 nm in radius and for five pairs in spur of 9 nm in radius. The differences between calculated TR EFE curves for concentrated solutions of TMPD are most noticeable ones for these two variants of spur structure. While modeling with these spur parameters fluorescence decays as well as TR MFE curves display smaller relative difference.

The plateau level of the TR EFE for 1 mM solution of TMPD at field strength of 24 kV/cm could not be reproduced for any parameters of the employed model. At low concentration of TMPD, the computer model predicts a very low amount of solute triplets. At the same time, an almost quantitative agreement between experiment and simulation can be attained assuming that the solution contains, in addition, about 10^{-5} M of electron acceptors that form stable radical anions, but have not as high electron affinity as to suppress the formation of ^{1}TMPD* upon recombination (Werst, 1996; Borovkov and Velizhanin, 2004). Formation of molecular radical anions having much lower mobility results in a sharp decrease of the rate of fluorescence quenching by external electric field.

This assumption is also consistent with the effect, which the addition of bromohexane has on the fluorescence of 1 mM solutions of TMPD (Fig. 1b). In the dilute solution with rather low contribution of TTA the difference between the effect of bromohexane and electric field be explained by electron transfer from radical anions of the suggested ‘‘weak’’ acceptors to bromohexane. This transfer would lead to additional fluorescence quenching. If such an impurity is introduced into calculation of TR EFE curves for low concentration of TMPD, then the optimal value of electron mobility increases up to 0.009–0.0095. The above-mentioned small amounts of impurity in the case of high concentration of TMPD have practically no effect on the calculation results.

There is another hypothetical possibility for explanation of the incomplete quenching of fluorescence from solutions with low concentration of TMPD by electric field. Although it is generally accepted that triplet-excited molecules of all alkanes decompose very quickly, in several picoseconds, these species have never been observed, and the lifetime of ^{3}S* has not yet been measured experimentally. It can be suggested, for example, that ^{3}S* have never been observed because of their poor optical absorption, while the actual lifetime of these species is not so short. In this case, ^{1}TMPD* can be formed in collisions of ^{3}TMPD* with triplet excited solvent molecules, and this channel would contribute at any concentration of TMPD.

4.4. Time-resolved magnetic field effect

Fig. 4 shows experimental and calculated curves of time-resolved magnetic field effect (TR MFE) for 1 and 20 mM solutions of TMPD in the field of 0.1 T. The presented model curves were calculated assuming that the rate of electron self-exchange reaction (11) involving radical cations of TMPD was $k_{11} = 5 \times 10^9\,\mathrm{M}^{-1}$/s. According to the modeling, this reaction accelerating phase relaxation is the only way to reproduce the increase in the magnetic field effect at times up to 100 ns with increasing concentration of TMPD. Direct manifestation of hyperfine interactions in TMPD$^{+\bullet}$ is unobservable because of the delay in the formation of TMPD$^{+\bullet}$, their self-exchange (11), and rather long fluorescence lifetime of TMPD. The tail of TR MFE curves is determined by spin-lattice relaxation of TMPD$^{+\bullet}$, which in a field of 0.1 T only weakly depends on the solute concentration. Spin-lattice relaxation time of primary solvent radical cations in these experiments is

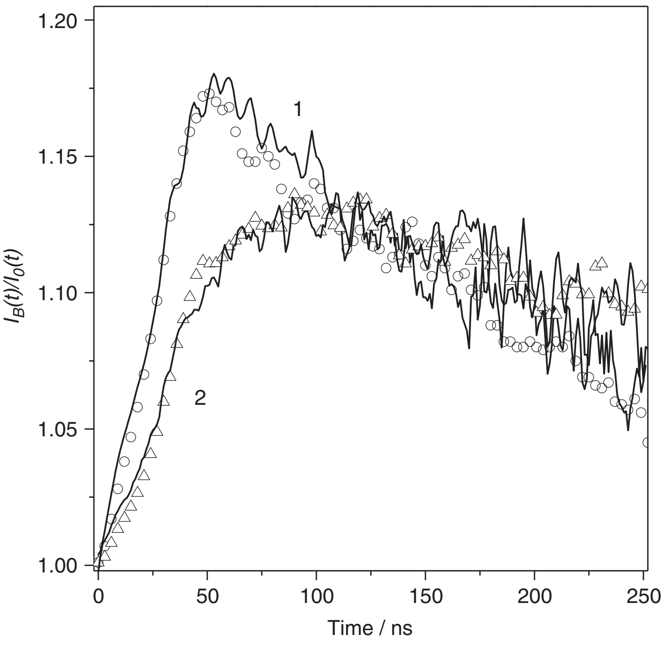

Fig. 4. Experimental (lines) and calculated (symbols) curves of time-resolved magnetic field effect for dodecane solutions of TMPD with concentration of 20 mM (curves 1) and 1 mM (curves 2) The calculated curves were obtained for four pair in spur of 5 nm in radius. Non-zero magnetic field in the experiment amounted to 0.1 T. Parameters of the modeling are given in Tables 1 and 2.

determined not very accurately, but the modeling shows that it is slightly shorter as compared to that for $\mathrm{TMPD}^{+\bullet}$.

If the main contribution to phase relaxation of spin-correlated ion pairs can be attributed to reactions (10) and (11), the mechanism of spin-lattice relaxation in $\mathrm{TMPD}^{+\bullet}$ remains unclear, since typical relaxation mechanisms cannot provide such s short relaxation time for an aromatic radical in solution (Bartels et al., 1985). It is also clear that the decay of the TR MFE curves cannot be explained by an increase of the fraction of magnetic-field-insensitive emission due to reaction (8), or contact interactions of radical cations $\mathrm{TMPD}^{+\bullet}$ with other species in the spur, as their frequency dramatically decreases after only several nanoseconds after formation of the pairs (Borovkov and Velizhanin, 2006). It is worth noting that long-range spin–spin dipole interactions cannot resolve the problem because in very similar conditions spin-relaxation time for radical ions of *para*-terphenyl is about 4 μs (Bagryansky et. al. 2000; Borovkov and Molin, 2004).

It is instructive for the method of TR MFE to discuss a meaning of "the fraction of radical ion pairs that are born in the singlet-correlated state" in a multiparticle spur (Brocklehurst, 1997; Anishchik et al., 1998; Bagryansky et al. 2000, 2004). The concept stated that the recombination rate of spin-correlated radical ion pairs amounts to nearly constant fraction of the rate for all the ion pairs. If fluorescence lifetime is very short, the approximation of "constant fraction of spin-correlated pairs" allows avoiding a detailed analysis of the geminate recombination kinetics (Bagryansky et al., 2000, 2004). Under these conditions TR MFE curve is given by the expression

$$\frac{I_B(t)}{I_0(t)}=\frac{\theta\rho_{\mathrm{ss}}^{B}(t)+\frac{1}{4}(1-\theta)}{\theta\rho_{\mathrm{ss}}^{0}(t)+\frac{1}{4}(1-\theta)}. \qquad (12)$$

Here θ denotes so-called fraction of spin-correlated radical ion pairs that give the fluorescence sensitive to magnetic field. Typically, the value of θ is varied within the range of 0.1–0.5 to fit the magnitude of experimental TR MFE curves. The spin state evolution in zero (0) and nonzero (B) magnetic fields as described by indexed $\rho_{\mathrm{ss}}(t)$ dependences is determined by the paramagnetic properties of radical ions involved (see Appendix A).

The weak dependence of the θ value on time was demonstrated earlier in computer experiment for track recombination of primary pairs $\mathrm{S}^{+\bullet}/e^-$ (Lozovoy et al., 1990). In charge acceptor solution the concept is equivalent to the requirement of nearly constant proportion between all the reaction rates $F_{\mathrm{g}}(t)$, $F_{\mathrm{c}}(t)$, $F_6(t)$, and $F_8(t)$, which appear in expression (A.8). Obviously, such proportion is absent and expression (12) is not valid at times where the process of energy transfer $F_6(t)$, which is approximately exponential in time dominates the other channels. Later, the fluorescence intensity is determined by diffusion-controlled reactions of ion recombination and TTA. At spur parameters, for which TR MFE curves from Fig. 4 were calculated, the fraction of geminate pairs $\mathrm{TMPD}^{+\bullet}/e^-$ among all secondary ion pairs becomes approximately constant (0.3–0.33) starting from 10 ns. In addition to cross-recombination, the magnitude of the magnetic field effect is decreased by TTA contribution, but both these channels have practically the same time dependency. This similarity allows one, in a proper time domain, to take into account all contributions, which are insensitive to magnetic field, with a single parameter θ. In this case this parameter concerns not only spur structure but also luminescent properties of the solutes used.

Finally, the example of TR MFE experiments is convenient for discussion why increasing the number of primary ion pairs to five requires a double increase in spur radius to keep the level of magneto-sensitive fluorescence the same. Magnetic field effects are determined by the relative contributions of geminate and cross pair recombination as well as triplet–triplet annihilation to delayed fluorescence. At not very high spur density, an increase in the number of primary ion pairs results in an increase of both cross recombination and TTA contributions that reduce magnetic field effect. To provide the same level of TR MFE curves one should increase spur radius to increase geminate recombination probability. Then the total probability of TTA is reduced but the yield of $^3\mathrm{D}^*$ is increased (Borovkov and Velizhanin, 2006). Eventually, when spur radius is increased, within the radius values and time domain under study, the TTA rate becomes higher as compared to the rate observed for smaller spur with the same ion pairs. This interplay between the different factors results in the need to increase the spur radius further to an unexpectedly large value.

5. Conclusions

The computer model of formation of excited molecular states in irradiated alkane solutions suggested in Borovkov and Velizhanin (2006) can reproduce the main features of experimentally observed kinetics of delayed fluorescence as well as the effects of the external fields. Modeling of delayed fluorescence decay curves from solutions of TMPD in dodecane in time range 0–250 ns shows that at times up to 40–50 ns the main contribution to the formation of singlet-excited TMPD molecules is the energy transfer from excited solvent molecules. At longer times the main channels for formation of $^1\mathrm{TMPD}^*$ are the recombination of pairs $\mathrm{TMPD}^{+\bullet}/e^-$ as well as the triplet–triplet annihilation of $^3\mathrm{TMPD}^*$ being formed within the same spur. The relative contribution of the second channel grows with the concentration of TMPD.

The results of modeling demonstrate that a track produced by 20-keV X-ray quanta in *n*-dodecane in the studied time range can be described by a set of isolated spherical spurs containing 4–5 ion pairs at the moment of formation. The radius of such an "effective" spur is about 5 nm for four pairs or 9–10 nm for five pairs.

Acknowledgment

The authors are grateful to Prof. V.F. Plyusnin and Dr. I. Pozdnyakov for their assistance in experiments on TTA rate constants determination and to Dr. F.B. Sviridenko and Dr. D.V. Stass for help in preparing of the publication. This work was supported by Russian Foundation for Basic Research (Grant 04-03-32161), and the program «Leading Science Schools» (Grant NS-5078.2006.3).

Appendix A

For a primary radical pair, which is assumed to be singlet initially, the evolution of the population of the singlet state in high $\rho_{ss}^{B}(t)$ and zero $\rho_{ss}^{0}(t)$ magnetic fields can be described by the following equations

$$\rho_{ss}^{B}(t) = \frac{1}{4} + \frac{1}{4}\,e^{-t/T_1} + \frac{1}{2}\,e^{-t/T_2}\,G_c^B(t)\,G_a^B(t), \tag{A.1}$$

$$\rho_{ss}^{0}(t) = \frac{1}{4} + \frac{3}{4}\,e^{-t/T_0}\,G_c^0(t)G_a^0(t), \tag{A.2}$$

where the indices a and c refer to the radical anion and the radical cation, respectively. $1/T_1 = 1/T_{1c} + 1/T_{1a}$ and $1/T_2 = 1/T_{2c} + 1/T_{2a}$ are the sums of the rates of spin-lattice and phase relaxation for radical cations and radical anions in high field, respectively. $1/T_0 = 1/T_{0c} + 1/T_{0a}$ is the parameter to describe phase relaxation in zero field. $G(t)$ is a function determined by hyperfine coupling constants and the g-factors of the radicals (Bagryansky et al., 2000).

If at time t' the initial radical cation $S^{+\bullet}$ is transformed into a secondary radical cation $D^{+\bullet}$, which is described by another spin-Hamiltonian, Eqs. (A.1) and (A.2) are to be replaced with the following equations:

$$\rho_{ss}^{B}(t,t') = \frac{1}{4} + \frac{1}{4}\,e^{-t'/T_{I1}}\,e^{-(t-t')/T_{II1}} + \frac{1}{2}\,e^{-t'/T_{I2}}\,e^{-(t-t')/T_{II2}}\,G_{Ic}^{B}(t')G_{IIc}^{B}(t-t')G_a^B(t), \tag{A.3}$$

$$\rho_{ss}^{0}(t,t') = \frac{1}{4} + \frac{3}{4}\,e^{-t'/T_{I0}}\,e^{-(t-t')/T_{II0}}\,G_{Ic}^{0}(t')G_{IIc}^{0}(t-t')G_a^0(t) \tag{A.4}$$

in high or zero magnetic fields, respectively. Here I and II refer to radical cations $S^{+\bullet}$ and $D^{+\bullet}$, respectively. In the present analysis, we assume that the contribution of the excess electron to spin dynamics can be neglected. As the solvent holes ($S^{+\bullet}$) are captured by solute with the quasi-first order rate constant k, the singlet state population at time t for the secondary geminate pairs can be found using the convolution of Eqs. (A.3) and (A.4) with exponential time distribution

$$\rho_{ss}(t) = k\int_0^t e^{-kt'}\rho_{ss}(t,t')\,dt'. \tag{A.5}$$

For the situations considered in this work, spin state dynamics in the radical pairs can be described in terms of the semiclassical approximation (Schulten and Wolynes, 1978) that gives for $G^0(t)$ and $G^B(t)$ functions of the form:

$$G^0(t) = \frac{1}{3}\left[1 + 2\left(1-\gamma^2\sigma^2t^2\right)e^{-\gamma^2\sigma^2t^2/2}\right], \tag{A.6}$$

$$G^B(t) = e^{e^{-\gamma^2\sigma^2t^2/2}}, \tag{A.7}$$

where σ^2 is the second moment of ESR spectrum of a radical.

ESR spectrum of n-dodecane radical cation in solution is an unresolved singlet with the second moment of the spectrum of about $\sigma_h = 0.6\,\text{mT}$, and these radicals are known to undergo the reaction of electron self-exchange with the rate that is substantially lower than the rate of diffusion encounters (Borovkov et al., 2002). Estimations reported in the cited work have showed that in n-hexane the electron self-exchange rate constant for the n-nonane radical cation was about $2\times10^8\,\text{M}^{-1}/\text{s}$. In more viscous dodecane, the same efficiency of encounters corresponds to the conditions of the intermediate rate of spectral exchange $(\gamma\sigma_h\tau_c)^2\approx0.3$, where τ_c is the electron exchange time. Because the exchange rate is rather high, we assumed that the inhomogeneous width of the ESR spectrum of $S^{+\bullet}$ can be neglected, and the only adjustable parameter was the phase relaxation time T_2. It was also assumed that the phase relaxation rate was independent of magnetic field, i.e., $T_2 = T_0$. It should be noted that in this case a better agreement between experimental and calculated curves was obtained.

Resolved ESR spectrum of $\text{TMPD}^{+\bullet}$ in alkane solution was not observed by the OD ESR method due to electron self-exchange (Werst, 1996), and so the spin state dynamics in the $D^{+\bullet}/e^-$ pairs was calculated using the semiclassical approximation with $\sigma_c = 1.43\,\text{mT}$ (Fisher, 1990). Furthermore, if reaction (11) is diffusion-controlled then even at the highest used concentration of TMPD the self-exchange provides a slow spectrum exchange. In this case, the rate of phase relaxation coincides with the rate of the self-exchange (Carrington and McLachlan, 1967; Schulten and Wolynes, 1978) since other relaxation mechanisms are likely to be insignificant (Bartels et al., 1985).

Expressions (A.3)–(A.7) were used to calculate spin dynamics of those spin-correlated pairs $D^{+\bullet}/e^-$, in which positive charge carrier $D^{+\bullet}$ was formed by electron transfer to solvent hole composing the geminate pair with this electron. For all other pairs the probability of forming singlet state was taken to be 0.25.

The simulated curves of TR MFE were found as the ratios of fluorescence kinetics $I_B(t)/I_0(t)$ as calculated in the following way:

$$I_{B,0}(t) = \frac{1}{\tau_{fl}}\int_{-\infty}^{t} dt'\,\exp\left(-\frac{t-t'}{\tau_{fl}}\right) \times \int_{-\infty}^{t'} dt''\left[F_g(t'-t'')\rho_{ss}^{B,0}(t'-t'') + \tfrac{1}{4}F_c(t'-t'') + F_6(t'-t'') + F_8(t'-t'')\right]g(t''). \tag{A.8}$$

Here $F_g(t)$ and $F_c(t)$ are the rate of recombination of geminate pairs and the rate of cross-recombination, respectively, τ_{fl} is fluorescence time of luminophor, $g(t) = \exp(-t^2/\delta^2)/(\pi\delta)^{1/2}$ is the function accounting for finite time resolution of the experimental setup ($\delta = 2\,\text{ns}$). The functions $F_6(t)$ and $F_8(t)$ are the kinetics of ^{1}TMPD* formation via reactions (6) and (8), respectively, which are controlled in the program.

References

Anishchik, S.V., Grigoryants, V.M., Shebolaev, I.V., Chernousov, Yu.D., Anisimov, O.A., Molin, Yu.N., 1989. Pulse X-ray fluorimeter with nanosecond time resolution. Pribory Techn. Eks. 4, 74–76 (in Russian).

Anishchik, S.V., Usov, O.M., Anisimov, O.A., Molin, Yu.N., 1998. Study of a fraction of spin-correlated pairs in radiation spurs by the methods of time-resolved magnetic field effects and quantum beats. Radiat. Phys. Chem. 51, 31–36.

Bagryansky, V.A., Usov, O.M., Borovkov, V.I., Kobzeva, T.V., Molin, Yu.N., 2000. Quantum beats in recombination of spin-correlated radical ion pairs with equivalent protons. Chem. Phys. 255, 237–245.

Bagryansky, V.A., Borovkov, V.I., Molin, Yu.N., 2004. Spectroscopic capabilities of the time-resolved magnetic field effect technique as illustrated in the study of hexamethylethane radical cation in liquid hexane. Phys. Chem. Chem. Phys. 6, 924–928.

Bartczak, W.M., Hummel, A., 1997. Computer simulation of charge recombination in model tracks of high-energy electrons in nonpolar liquids; kinetics and escape. Radiat. Phys. Chem. 49 (6), 675–687.

Bartels, D.M., Lawler, R.G., Trifunac, A.D., 1985. Electron T_1 measurements in short-lived free radicals by dynamic polarization recovery. J. Chem. Phys. 83 (6), 2686–2707.

Blum, F.D., Pickup, S., Ninham, B., Chen, S.J., Evans, D.F., 1985. Structure and dynamics in three-component microemulsions. J. Phys. Chem. 89 (4), 711–713.

Bondi, A., 1964. van der Waals volumes and radii. J. Phys. Chem. 68, 441–451.

Borovkov, V.I., Velizhanin, K.A., 2004. A novel approach to study radical ion reactions in the course of geminate recombination by the quenching of time-resolved delayed fluorescence. Chem. Phys. Lett. 394, 441–445.

Borovkov, V.I., Velizhanin, K.A., 2006. The effect of encounters involving ions, excited molecules, and neutral radicals in a track on the delayed fluorescence of irradiated alkane solutions. Radiat. Phys. Chem., in press, doi:10.1016/j.radphychem.2006.09.008.

Borovkov, V.I., Anishchik, S.V., Anisimov, O.A., 1995. Time-resoved electric field effects in recombination fluorescence. High Energy Chem. 29, 401.

Borovkov, V.I., Anishchik, S.V., Anisimov, O.A., 1997. Time-resoved electric field effects in recombination fluorescence as a method of studying primary radiation-chemical processes. Chem. Phys. Lett. 270, 327–332.

Borovkov, V.I., Bagryansky, V.A., Yeletskikh, I.V., Molin, Yu.N., 2002. Radical cations of *n*-alkanes in irradiated solutions as studied by time-resolved magnetic field effects. Mol. Phys. 100, 1379–1384.

Borovkov, V.I., Anishchik, S.V., Anisimov, O.A., 2003. Mobility of geminate radical ions in concentrated alkane solutions as measured using electric field dependence of delayed fluorescence. Radiat. Phys. Chem. 67, 639–650.

Borovkov, V.I., Molin, Yu.N., 2004. Paramagnetic relaxation of cyclohexane radical cation in solution as measured by the method of time-resolved magnetic field effect. Phys. Chem. Chem. Phys. 6, 2119–2124.

Brocklehurst, B., 1992a. Model calculation on hydrocarbon radiolysis. Part 1—Spin correlation effects in pure alkanes. J. Chem. Soc. Faraday Trans. 88 (2), 167–175.

Brocklehurst, B., 1992b. Model calculation on hydrocarbon radiolysis. Part 2—Excited states in solutions of aromatics in alkanes. J. Chem. Soc. Faraday Trans. 88 (9), 2823–2832.

Brocklehurst, B., 1997. Spin correlated and magnetic field effects in radiolysis. Radiat. Phys. Chem. 50, 213–225.

Carmichael, I., Hug, G.L., 1986. Triplet–triplet absorption spectra of organic molecules in condensed phase. J. Phys. Chem. Ref. Data 15, 1–250.

Carrington, A., McLachlan, A.D., 1967. Introduction to Magnetic Resonance with Application to Chemistry and Chemical Physics. Harper & Row, Publishers, NewYork, Evanston, and London.

Doktorov, A.B., Burstein, A.I., 1975. Quantum theory of the distant electron transfer accelerated by diffusion. JETP (Sov.) 68, 1349–1362 (in Russian).

Fisher, H. (Ed.), 1990. Landolt-Börnstein. Numerical data and functional relationship in science and technology, new series. group II. Atomic and molecular physics. vol. 17: Magnetic Properties of Free Radicals. Subvolume h. Organic cation radicals. Bi- and polyradicals. Index of substances for volumes II/1,II/9, and II/17. Springer-Ferlag, Berlin, Heidelberg, New York.

Gee, N., Freeman, G.R., 1987. Electron mobilities, free ion yeilds, and electron thermalization distances in liquid long-chain hydrocarbons. J. Chem. Phys. 86, 5716–5721.

Grampp, G., Jaenicke, W., 1984. ESR-investigation of the homogenious electron transfer reactions between substituted *p*-phenylenediamines and quinonediamines, and the validity of Marcus' theory. I. Measurement at 293 K. Ber. Bunsenges. Phys. Chem. V. 88, 325–334.

Grivin, V.P., Plyusnin, V.F., Khmelinski, I.V., Bazhin, M., Mitewa, M., Bontchev, P.R., 1990. Pulsed laser photolysis of the $PtCl_6^{2-}$creatinine system in methanol. J. Photochem. Photobiol. A.: Chem. 51 (13), 371–377.

Heisel, F., Miehe, J.A., 1982. Intermolecular transfer and quenching of electronic excitation energy in fluid solution: Interpretation of experimental data with a diffusion model including distance dependent interaction. J. Chem. Phys. 77, 2558–2569.

Holroyd, R.A., Nishikawa, M., 2002. Pressure effects on electron reactions and mobility in nonpolar liquids. J. Phys. Chem. 89, 2909–2913.

Holroyd, R.A., Sham, T.K., 1985. Ion yields in hydrocarbon liquids exposed to X-rays of 5–30 energy. Radiat. Phys. Chem. 51 (1), 37–43.

Holroyd, R.A., Preses, J.M., Hanson, J.C., 1997. Excited singlet-state yields in hydrocarbon liquids exposed to X-rays. J. Phys. Chem. A 101, 6931–6935.

Hummel, A., 1987. Single-pair diffusion model of radiolysis of hydrocarbon liquids. In: Freeman, G.R. (Ed.), Kinetics of Nonhomogeneous Processes. Wiley, New York, pp. 215–275.

Klein, J., Voltz, R., 1977. Time resolved magnetic modulation of ion recombination in organic solution: spin motion in radical ion pairs. Can. J. Chem. 55, 2102–2106.

Kondratyev, V.N. (Ed.), 1974. Energy of Chemical Bonds, Ionization Potentials and Electron Affinities. Nauka, Moscow, p. 351pp (in Russian).

Kowert, B.A., Dang, N.C., Sobush, K.T., Seele III, L.G., 2001. Diffusion of aromatic hydrocarbons in *n*-alkanes and cyclohexanes. J. Phys. Chem. A 107, 4790–4795.

Kowert, B.A., Sobush, K.T., Fuqua, C.F., Mapes, C.L., Jones, J.B., Zahm, J.A., 2003. Size-dependent diffusion in the *n*-alkanes. J. Phys. Chem. A 107, 4790–4795.

LaVerne, J.A., Pimblott, S.M., Wojnarovits, L., 1997. Diffusion-kinetic modeling of γ-radiolysis of liquid cycloalkanes. J. Phys. Chem. A 101 (8), 1628–1634.

Lissi, E.A., Encinas, M.V., 1989. Representative kinetic behavior of selected reaction intermediates: Triplet states. In: Scaiano, J.C. (Ed.), CRC Handbook of Organic Photochemistry, vol. II. CRC Press, Inc., Boca Raton, pp. 111–176.

Lozovoy, V.V., Anishchik, S.V., Medvedev, N.N., Anisimov, O.A., Molin, Yu.N., 1990. Monte Carlo modeling of radical ion recombination in multiparticle tracks. Chem. Phys. Lett. 167, 122–128.

Mehnert, R., Brede, O., Naumann, W., Hermann, R., 1988. The mechanism of singlet energy transfer from alkanes. Radiat. Phys. Chem. 32 (3), 325–328.

Nakamura, S., Kanamaru, N., Nohara, S., Nakamura, H., Saito, Y., Tanaka, J., et al., 1984. The photoionization mechanism of *N,N,N′,N′*-tetramethyl-*p*-phenylenediamine in acetonitrile. Bull. Chem. Soc. Jpn. 57, 145–150.

Okamoto, M., Teratsuji, T., Tazuke, Y., Hirayama, S., 2001. Effect of pressure on intersystem crossing between the encounter complex pairs involved in triplet–triplet annihilation of 2-acetonaphthone in liquid solution. J. Phys. Chem. A 105 (18), 4574–4578.

Potashnik, R., Ottolenghi, M., Bensasson, R., 1969. Photoionization and delayed fluorescence in liquid solutions of *N,N,N′,N′*-tetramethyl-*p*-phenylenediamine. J. Phys. Chem. 73 (6), 1912–1918.

Rothman, W., Hirayama, F., Lipsky, S., 1973. Fluorescence of saturated hydrocarbons. III. Effect of molecular structure. J. Chem. Phys. 58 (4), 1300–1317.

Saeki, A., Kozawa, T., Yoshida, Y., Tagawa, S., 2001. Study of geminate ion recombination in liquid dodecane using pico- and subpicosecond pulse radiolysis. Radiat. Phys. Chem. 60, 319–322.

Sauer Jr., M.C., Jonah, C.D., 1994. The ratio of triplet to singlet excited state formation from ion recombination in the radiolysis of aromatic solutes in alkane liquids. Radiat. Phys. Chem. 44, 281–295.

Sauer Jr., M.C., Jonah, C.D., Naleway, C.A., 1991. Study of the reactions of geminate ions in irradiated scintillator, hydrocarbon solutions using recombination fluorescence and stochastic simulations. J. Phys. Chem. 95, 730–740.

Shinsaka, K., Koizumi, H., Yoshimi, T., Kouchi, N., Nakamura, Y., Toriumi, M., et al., 1985. Fluorescence lifetimes and excitation spectra of liquid alkanes measured by means of synchrotron radiation. J. Chem. Phys. 83 (9), 4405–4409.

Schmidt, K.H., 1983. DC conductivity and geminate ion recombination in irradiated hydrocarbons: model calculation. Chem. Phys. Lett. 103, 129–132.

Schmidt, W.F., 1977. Electron mobility in nonpolar liquids: the effect of molecular structure, temperature, the electric field. Can. J. Chem. 55, 2197–2210.

Schmidt, W.F., 1997. Liquid State Electronics of Insulating Liquids. CRC Press, Boca Raton, New York.

Schmidt, W.F., Allen, A.O., 1970. Free-ion yields in sundry irradiated liquids. J. Chem. Phys. 52 (5), 2345–2351.

Schmidt, K.H., Sauer Jr., M.C., Lu, Y., Liu, A., 1990. Quantum yields of photoionization in 308-nm two-photon ionization of solutes in hydrocarbon solutions and their relationship to the observed conductivity signals. J. Phys. Chem. 94 (1), 244–251.

Schulten, K., Wolynes, P.G., 1978. Semiclassical description of electron spin motion in radicals including the effect of electron hopping. J. Chem. Phys. 68, 3292–3297.

Schwarz, F.P., Smith, D., Lias, S.G., Ausloos, P., 1981. The fluorescence and photofragmentation of liquid saturated hydrocarbons at energies above the photoionization threshold. J. Chem. Phys. 75 (8), 3800–3808.

Terazima, M., 2000. Is the translational diffusion of organic radicals different from that of closed-shell molecules? Acc. Chem. Res. 33, 687–694.

Terazima, M., Okazaki, T., Hirota, N., 1995. Translational diffusion process of charged radicals: *N,N,N′,N′*-tetramethyl-*p*-phenylenediamine and its cation radical. J. Photochem. Photobiol. A: Chem. 92, 7–12.

Ukai, A., Hirota, N., Terazima, M., 2000. Diffusion of organic molecules in the excited triplet states detected by the transient grating with a high wavenumber. J. Phys. Chem. A 104 (29), 6681–6688.

Veselov, A.V., Anisimov, O.A., Molin, Y.N., 1991. Time-resolved single-photon counting technique in radiolysis of hydrocarbons. In: Tabata, Y. (Ed.), Pulse Radiolysis. CRC press, Boca Raton, pp. 27–51.

Werst, D.W., 1996. Self-exchange reactions of radical anions in *n*-hexane. Chem. Phys. Lett. 251, 315–322.

Werst, D.W., Bakker, M.G., Trifunac, A., 1990. The fate of alkane radical cation in liquid and solid hydrocarbons. Time-resolved fluorescence detected magnetic resonance. J. Am. Chem. Soc. 112 (1), 40–50.